

# Northumbria Research Link

Citation: Narayana, Mahinsasa, Putrus, Ghanim, Jovanovic, Milutin, Leung, Pak Sing and McDonald, Stephen (2012) Generic maximum power point tracking controller for small-scale wind turbines. *Renewable Energy*, 44. pp. 72-79. ISSN 0960-1481

Published by: Elsevier

URL: <http://dx.doi.org/10.1016/j.renene.2011.12.015>  
<<http://dx.doi.org/10.1016/j.renene.2011.12.015>>

This version was downloaded from Northumbria Research Link:  
<https://nrl.northumbria.ac.uk/id/eprint/6489/>

Northumbria University has developed Northumbria Research Link (NRL) to enable users to access the University's research output. Copyright © and moral rights for items on NRL are retained by the individual author(s) and/or other copyright owners. Single copies of full items can be reproduced, displayed or performed, and given to third parties in any format or medium for personal research or study, educational, or not-for-profit purposes without prior permission or charge, provided the authors, title and full bibliographic details are given, as well as a hyperlink and/or URL to the original metadata page. The content must not be changed in any way. Full items must not be sold commercially in any format or medium without formal permission of the copyright holder. The full policy is available online: <http://nrl.northumbria.ac.uk/policies.html>

This document may differ from the final, published version of the research and has been made available online in accordance with publisher policies. To read and/or cite from the published version of the research, please visit the publisher's website (a subscription may be required.)



**Northumbria  
University**  
NEWCASTLE



University**Library**

# Generic Maximum Power Point Tracking

## Controller for Small Scale Wind Turbines

M. Narayana<sup>1</sup>, G. A. Putrus<sup>1</sup>, M. Jovanovic<sup>1</sup>, P. S. Leung<sup>1</sup> and S. McDonald<sup>2</sup>

<sup>1</sup> Northumbria University, Ellison Place, Newcastle upon Tyne, UK

[mahinsasa@yahoo.com](mailto:mahinsasa@yahoo.com), [ganim.putrus@unn.ac.uk](mailto:ganim.putrus@unn.ac.uk), [milutin.jovanovic@unn.ac.uk](mailto:milutin.jovanovic@unn.ac.uk) and  
[ps.leung@unn.ac.uk](mailto:ps.leung@unn.ac.uk)

<sup>2</sup> New and Renewable Energy Centre (NaREC), Blyth, UK

[steve.mcdonald@narec.co.uk](mailto:steve.mcdonald@narec.co.uk)

**Abstract--**The output power of a wind energy conversion system (WECS) is maximized if the wind rotor is driven at an optimal rotational speed for a particular wind speed. To achieve this, a Maximum Power Point Tracking (MPPT) controller is usually used. A successful implementation of the MPPT controller requires knowledge of the turbine dynamics and instantaneous measurements of the wind speed and rotor speed. To obtain the optimal operating point, rotor-generator characteristics should be known and these are different from one system to another. Therefore, there is a need for an efficient universal MPPT controller for WECS to operate without predetermined characteristics. MPPT control of WECSs becomes difficult due to fluctuation of wind speed and wind rotor inertia. This issue is analyzed in the paper, and an Adaptive Filter together with a Fuzzy Logic based MPPT controller suitable for small-scale WECSs is proposed. The proposed controller can be implemented without predetermined WECS characteristics.

**Index Terms--**Wind energy conversion systems, Wind rotor, Maximum power point tracking control, Adaptive Control, Fuzzy Logic.

## 1. Nomenclature

$\Delta d$	“Fuzzy set” output
$\eta_{opt}$	Optimal generator efficiency
$\Phi_d, \Phi_q$	d-q axis flux linkages
$\lambda$	Tip speed ratio
$\rho$	Air density
$\omega$	Angular velocity of the wind rotor
$\omega_s$	Angular frequency of the stator voltage
$C_p$	Power coefficient of the wind rotor
$C_{p\_opt}$	Power coefficient at optimal operating condition
$C_t$	Torque coefficient
D	Duty ratio (range, 0 to 1)
$i_{d,q}$	PMG stator d-q currents
$V_G$	The voltage at the generator side
$I_G$	The current flow from the generator side
$V_B$	The voltage at the d.c. bus
$I_B$	The current flow towards the d.c. bus
J	Momentum of inertia of rotating parts
$L_{d,q}$	3-phase d-q inductances

$P_a$	Aerodynamic power captured by the wind rotor
$P_E$	Output power of the WECS generator
$P_l$	Electrical and friction losses
$P_{WR}$	Power delivered by the wind rotor to the generator
PMG	Permanent Magnet Generator
$R$	Generator winding resistance
$R_r$	Radius of the wind rotor
$T_e$	Electromagnetic torque of the PMG
$T_{friction}$	Torque due to system friction losses
$u_{d,q}$	PMG stator d-q voltages
$v$	Incident wind speed
VSFP	Variable-speed Fixed-Pitch
WECS	Wind Energy Conversion System

## 2. Introduction

Variable-speed fixed-pitch (VSFP) wind energy conversion systems (WECSs) are generally more efficient compared to fixed-speed counterparts, and hence are becoming increasingly popular, particularly in small-scale applications. Wind turbines with variable-pitch control are generally costly and complex. Typically, variable-speed wind turbines are aerodynamically controlled, usually by using power electronics, to regulate the torque and speed of the turbine in order to maximize the output power. Therefore, VSFP approach is becoming more popular for low cost construction, and is the most common scheme for small wind turbines. In this scheme,

a Maximum Power Point Tracker (MPPT) is used to control the restoring torque of the electrical generator for optimum system operation [1]. Accordingly, the performance of a VSFP wind turbine could be optimized without the need for a complex aerodynamic control. The maximum output power from the turbine is usually obtained by controlling the system such that the relevant points of wind rotor curve and electrical generator operating characteristic coincide. In order to achieve this, it is necessary to drive the turbine at optimal rotor speeds for a particular wind speed profile.

Techniques that employ wind sensors generally perform well with wind speed variations, as the control system responds to variation in wind conditions [2, 3]. However, in practice it is difficult to accurately measure the wind speed by an anemometer installed close to the wind turbine, as the latter is exposed to different forces due to wake rotation. Normally, wind rotor blades experience conning and flapping effects due to wind forces. Wind speed varies across the swept area of the wind rotor as a result of the yaw behavior. Accordingly, wind rotor dynamics vary and become difficult to predict in real systems. Therefore, it would be useful to implement a sensorless control strategy, which is proposed in this study, for small scale wind turbine systems that operate without predetermined turbine characteristics.

### **3. Aerodynamic Characteristics of the Wind Rotor**

Based on the wind turbine aerodynamic behavior, the amount of power that a wind turbine can capture from the kinetic energy contained in the wind is given as [4]:

$$P_a = \frac{1}{2} \cdot \rho \cdot \pi \cdot R_r^2 \cdot v^3 \cdot C_p \quad (1)$$

Where  $P_a$  is the captured power by the wind rotor,  $\rho$  is the air density ( $\text{kg}/\text{m}^3$ ),  $R$  is the

radius of the rotor (m) and  $v$  is the speed of the incident wind (m/s).  $C_p$  is the power coefficient which for a given wind rotor depends on the pitch angle of the wind rotor blades and on the tip speed ratio ( $\lambda$ ) defined as:

$$\lambda = \frac{\omega \cdot R_r}{v} \quad (2)$$

where  $\omega$  is the angular velocity of the rotor (rad/s).

The wind rotor aerodynamic characteristics are usually represented by the  $C_p - \lambda$  relationship, as shown in Fig. 1. Note that  $C_p$  is maximum at a certain value of tip speed ratio  $\lambda_{opt}$  (optimal ratio) which results in a maximum power extraction. For variable speed WECSSs, when wind speed varies, the rotor speed should be adjusted to follow the optimum operating point for maximum power generation.

Using (1) and (2), the aerodynamic torque ( $T_a$ ) of a wind rotor can be obtained as:

$$T_a = \frac{P_a}{\omega} = \frac{1}{2} \cdot \rho \cdot \pi \cdot R_r^3 \cdot v^2 \cdot \frac{C_p}{\lambda} \quad (3)$$

$$T_a = \frac{1}{2} \cdot \rho \cdot \pi \cdot R_r^3 \cdot v^2 \cdot C_t, \quad (4)$$

where  $C_t = \frac{C_p}{\lambda}$  is the torque coefficient and is plotted in Fig. 1 together with  $C_p$ .

Note that maximum (optimum)  $C_p$  and  $C_t$  occur at different  $\lambda$  values.

The aerodynamic torque of a wind rotor is a function of wind speed ( $v$ ) and rotational speed ( $\omega$ ) of the rotor [5]. For a wind turbine-generator system with a gearbox, the mechanical torque (input to the generator) can be expressed as  $T = K \cdot f(v, \omega)$  where  $K$  is the gear ratio.

$$T = K \cdot f(v, \omega) \quad (5)$$

For small scale wind turbine generators, there is no gearbox and hence K=1.

**Fig. 1. Wind rotor characteristics**

#### 4. Mathematical Modelling of Permanent-Magnet Generators

Permanent-magnet generators (PMGs) are self-excited and have low maintenance requirements afforded by brushless design. Hence, they are appropriate and widely used for small-scale wind turbines where the cost of magnets is not such a prohibiting factor as with large turbine generators [6, 7].

Permanent-magnet generators are usually modelled assuming uniform distribution of stator 3-phase windings, electrical and magnetic symmetry, unsaturated magnetic circuit and negligible iron losses. A simple model of the generator can be obtained by conversion from  $(a,b,c)$  to  $(d,q)$  coordinates which is realized by means of the Park Transform [8]. This gives [9, 10];

$$u_d = Ri_d + L_d \frac{di_d}{dt} - \Phi_q \omega_s \quad (6)$$

$$u_q = Ri_q + L_q \frac{di_q}{dt} + \Phi_d \omega_s \quad (7)$$

where  $u_{d,q}$  are the stator  $d,q$  voltages,  $R$  is the stator winding resistance,  $L_{d,q}$  are the 3 phase  $d,q$  inductances,  $i_{d,q}$  are the  $d,q$  currents,  $\Phi_d, \Phi_q$  are the  $d,q$  flux linkages, and  $\omega_s$  is the angular frequency of the stator voltage.

Also,

$$\Phi_d = L_d i_d + \Phi_m \quad (8)$$

$$\Phi_q = L_q i_q \quad (9)$$

where,  $\Phi_m$  is the constant flux due to the permanent magnets. Thus, (6) and (7)

become:

$$u_d = Ri_d + L_d \frac{di_d}{dt} - L_q i_q \omega_s \quad (10)$$

$$u_q = Ri_q + L_q \frac{di_q}{dt} + (L_d i_d + \Phi_m) \omega_s \quad (11)$$

The electromagnetic torque of a  $p$ -pole machine is obtained as[9];

$$T_e = p(\Phi_d i_q - \Phi_q i_d) = p[\Phi_m i_q + (L_d - L_q)i_d i_q] \quad (12)$$

where;  $p$  is number of pole pairs.

If the permanent magnets are uniformly mounted on the rotor surface, then  $L_d$  and  $L_q$  may be assumed equal and the electromagnetic torque becomes [11];

$$T_e = p\Phi_m i_q \quad (13)$$

Note that the stator voltage frequency ( $\omega_s$ ) is proportional to the shaft rotational speed ( $\omega$ ), i.e.  $\omega_s = p\omega$

The electromagnetic torque developed by the generator is a function of the generator current ( $I_G$ ), magnetic flux linkage and number of pole pairs [12, 13]. For a particular generator, the magnetic flux linkage and number of pole pairs are fixed parameters.

Hence,  $T_e \propto I_G$ . Therefore, the electromagnetic torque of a generator ( $T_e$ ) can be varied by controlling the PMG current. The main power loss in the PMG may be expressed as  $3 \cdot I_G^2 R$ . This loss increases at higher torques (as  $I_G$  is higher) and this operation is associated with low rotational speed and low voltage for the same output power. Therefore, variation of the power loss needs to be considered for maximum power tracking, as described in the following section.

## 5. Control Strategies

The inherent wind rotor characteristics shown in Fig. 1 indicate that maximum torque is delivered by the wind rotor at a lower rotational speed as compared to that for maximum aerodynamic power point. Also, the PMG loss varies with the level of torque transmitted through the system. Therefore, optimum operation does not occur at the maximum points of the wind rotor aerodynamic power curves, but at the maximum points of the electrical output power curve, as shown in Fig. 2. Consequently in order to obtain maximum power output, the restoring power curve of the generator (shown in Fig.2) need to be adjusted to tally with the actual maximum operating point of the PMG output power curve. This is usually done by varying the generator load.

For optimal operation of the WECSs, aerodynamic power utilization needs to be maximized whilst system losses are kept at minimum level. The operating point of the maximum aerodynamic power and the operating point of minimum system losses are not the same. Therefore, the effective power ( $P$ ) of the system, which is defined in this study as the difference of the aerodynamic power ( $P_a$ ) and the system losses ( $P_l$ ), is to be maximized for optimal operation of the system. The effective power versus rotational speed curves for two wind speed conditions  $V_1$  and  $V_2$  are shown in Fig. 3. As can be seen, for optimum operation of the wind turbine, if the wind speed varies from  $V_1$  to  $V_2$ , the wind rotor speed should be changed from  $\omega_1$  to  $\omega_2$ . However, due to the turbine inertia, the rotor speed of the wind turbine cannot change instantly or as fast as the change in wind speed or direction.

**Fig. 2. Operating point of the wind power system**

MPPT controllers usually employ wind speed sensors (anemometers) to provide a feedback reference signal to the MPPT controller to set the turbine speed. MPPT control may also be implemented using a sensor-less control , where the generator output frequency and power (or torque) mapping techniques are used to track the MPP [14]. Another method for MPPT uses the output power of the PMG as a feedback signal in a “perturbation & observation” algorithm, which is used to find the maximum power point. This “searching” method does not require knowledge of system parameters which makes it suitable for small wind turbines [15, 16]. However, in dynamic conditions, the stored energy of rotating parts varies and tracking of the MPP using the “searching” method becomes difficult as the MPP is not steady.

**Fig. 3. Function of MPPT mechanism**

## 6. Power Flow in the Wind Turbine System

Power flow in a wind turbine system is represented in Fig. 4. During dynamic conditions ( $\dot{\phi} \neq 0$ ), the mechanically stored energy of rotating parts is variable and this makes it difficult to track the MPP (e.g. by using hill-climbed searching methods) from the electric power as the electrical power output is uncorrelated with the captured aerodynamic power by the wind rotor. The aerodynamic torque ( $T_a$ ) under dynamic conditions is given as:

$$T_a = \dot{\phi}J + T_e + T_{friction} \quad (14)$$

where  $J$  is moment of inertia of rotating parts,  $T_e$  is the electromagnetic torque of the generator and  $T_{friction}$  is the torque due to system friction losses.

Equation (14) may be rewritten as:

$$P_a = \omega \cdot \dot{\omega} \cdot J + P_E + P_l \quad (15)$$

$$P_{WR} = P_a - \omega \cdot \dot{\omega} \cdot J \quad (16)$$

$$P_E = P_{WR} - P_l \quad (17)$$

where  $P_a$  is the aerodynamic power extracted by the rotor,  $P_{WR}$  is power delivered by the wind rotor to the generator (see Fig. 4),  $P_E$  is the output power of the generator,  $P_l$  is the electrical and friction losses and  $\dot{\omega} = d\omega/dt$ .

Therefore;

$$P_E = -\omega \cdot \dot{\omega} \cdot J + (P_a - P_l) \quad (18)$$

This equation defines the relationship, during dynamic conditions, between the electrical output power of the generator ( $P_E$ ), the aerodynamic power extracted by the rotor ( $P_a$ ) and the mechanically stored energy of rotating parts. In this study, an adaptive filter is used to extract the values of ( $\omega \cdot \dot{\omega} \cdot J$ ) and ( $P_a - P_l$ ) from the measured values of electrical output power, as described in the following section. The extracted signals are then used as control signals for the proposed MPPT to define the optimum operating points.

## 7. Adaptive Filtering

Wind speed-time series data typically exhibit autocorrelation, which can be defined as the degree of dependence on preceding values [17]. Therefore, variation of mechanically stored energy in the rotating parts ( $\omega \cdot \dot{\omega} \cdot J$ ) and electrical output ( $P_E$ ) are time series data. Variation of the rotational speed is mainly dependent on the momentum of inertia of the rotating parts. As given by (18), the electrical output of the generator is the combination of the effective output power ( $P_a - P_l$ ) and the variation of mechanically stored energy. Accordingly, the wind rotor speed and

effective output power of the WECS change with the wind speed variations.

In this work, a simulation study (based on real wind data) was used to examine the correlation between the time series data of  $(\omega \cdot \dot{\omega})$  and electrical output. A small wind turbine at the National Engineering Research & Development Centre (NERDC) in Sri Lanka was simulated in MATLAB/SIMULINK using measured (actual) wind speed data in turbulent wind conditions. Specifications of the system used are given in the Appendix (A).

An “adaptive filter” is a filter that self-adjusts its transfer function according to an optimizing algorithm. The adaptive filter,  $W$ , is implemented using the least mean-square algorithm. A block diagram of the filter is shown in Fig. 5. An error signal,  $e(n)$ , is computed as  $e(n) = d(n) - y(n)$ , which measures the difference between the output of the adaptive filter [ $y(n)$ ] and the output of an unknown system [ $d(n)$ ]. With reference to Fig 5 and assuming that,  $p(n)$  is uncorrelated with  $u(n)$ ,  $z(n)$  and  $y(n)$ , and  $u(n)$ ,  $z(n)$ ,  $y(n)$  are statistically stationary and have zero means.

$$e(n) = p(n) + z(n) - y(n) \quad (19)$$

Squaring of both sides of (19):

$$e(n)^2 = p(n)^2 + [z(n) - y(n)]^2 + 2p(n)[z(n) - y(n)] \quad (20)$$

**Fig. 4. Power flow of the wind turbine**

Taking expectation of both sides of (20), and realizing that  $p(n)$  is uncorrelated with  $z(n)$  and  $y(n)$

$$\begin{aligned} E[e(n)^2] &= E[p(n)^2] + E[z(n) - y(n)]^2 + 2E[p(n)[z(n) - y(n)]] \\ &= E[p(n)^2] + E[z(n) - y(n)]^2, \end{aligned} \quad (21)$$

as  $E[z(n)] = 0$  and  $E[y(n)] = 0$

Adapting the filter to minimize  $E[e(n)^2]$  will not affect the signal power  $E[p(n)^2]$ .

Accordingly, the minimum output signal power is,

$$E_{\min}[e(n)^2] = E[p(n)^2] + E_{\min}\{[z(n) - y(n)]^2\} \quad (22)$$

The signal power  $E[p(n)^2]$  is unchanged when the filter coefficients are adjusted in error minimization algorithm. Consequently, only the term  $E\{[z(n) - y(n)]^2\}$  is minimized in the mean square error (MSE) minimization. When the algorithm converges to minimum mean square error (MMSE) solution,  $y(n)$  represents the best estimation of  $z(n)$  [18].

Thus  $z(n) \approx y(n)$  since  $e(n) = p(n) + z(n) - y(n)$ . This implies  $e(n) \approx p(n)$ , where  $p(n)$  is the best estimate of the error signal  $e(n)$ . This argument implies that minimization of MSE entails.

If  $X(t)$  and  $Y(t)$  are two sets of time series data, the correlation coefficient  $r_{X,Y}$  between them is given as;

$$\text{Correlation}(X, Y) = r_{XY}$$

$$= \frac{\sum_{t=1}^N (X(t) - \bar{X})(Y(t) - \bar{Y})}{\sqrt{\sum_{t=1}^N (X(t) - \bar{X})^2 \sum_{t=1}^N (Y(t) - \bar{Y})^2}} \quad (23)$$

$$\text{where } \bar{X} = \frac{\sum_{t=1}^N X(t)}{N} \quad \text{and, } \bar{Y} = \frac{\sum_{t=1}^N Y(t)}{N}$$

Using 2500 data sets obtained from the simulation study, the correlation coefficients between the time series data  $(\omega \cdot \dot{\omega})$  and  $(\omega \cdot \dot{\omega} \cdot J)$  in addition to  $(\omega \cdot \dot{\omega})$  and  $P_E$  were determined as;

$$\text{correlation}[(\omega \cdot \dot{\omega}), (\omega \cdot \dot{\omega} \cdot J)] = 1$$

$$\text{correlation}[(\omega \cdot \dot{\omega}), P_E] = 0.3822$$

The signal  $(\omega \cdot \dot{\omega})$  is highly correlated with variation of mechanically stored energy  $(\omega \cdot \dot{\omega} \cdot J)$  and weakly correlated with electrical output power  $(P_E)$ . The signal of variation of mechanically stored energy  $(\omega \cdot \dot{\omega} \cdot J)$  has zero mean. Therefore, an adaptive filter in noise cancellation mode can be utilized to filter the effective power  $(P_a - P_l)$  from the signal of electrical power  $(P_E)$  output [19].

On the basis of this error, the adaptive filter changes its coefficients in an attempt to reduce the error. The input signals to the adaptive filter are the electrical power output  $(P_E)$  and  $(\omega \cdot \dot{\omega})$ .

Referring to Fig. 5;

$$u(n) = -\omega \dot{\omega}, \quad Z(n) = -\omega \dot{\omega} \cdot J \quad \text{and} \quad d(n) = P_E.$$

$$d(n) = P(n) + Z(n)$$

$$y(n) = \sum_{k=0}^{N-1} W(k) u(n-k) \quad (24)$$

$$\text{Where} \quad W = \begin{bmatrix} W(0) \\ W(1) \\ \vdots \\ W(N-1) \end{bmatrix}$$

$$y(n) = W^T (n-1) u(n) \quad (25)$$

$$e(n) = d(n) - y(n) \quad (26)$$

$$W(n) = W(n-1) + f(e(n), u(n), \mu) \quad (27)$$

where  $f(e(n), u(n), \mu)$  is the weight update function and  $\mu$  is the adaptation step size.

### **Fig. 5. Function of the Adaptive filtering system**

A Least Mean Square (LMS) algorithm was used to estimate the weights of the filter [19, 20]. In this study, an adaptive system with a length of 16 elements was used to identify the input control signals. The outputs of the adaptive filter are;

$$Z(n) = -\omega \cdot \dot{\omega} \cdot J \text{ and } P(n) = P_a - P_l.$$

Performance of the adaptive filter when used with the NERDC wind turbine system is illustrated in Fig. 6 where the calculated effective power and variation of mechanically stored energy are compared with the outputs of the adaptive system. Simulation results show that  $P_a - P_l$  and  $(\omega \cdot \dot{\omega} \cdot J)$  signals can be extracted from the input signals  $P_E$  and  $(\omega \cdot \dot{\omega})$  with reasonable accuracy. Therefore, by using an adaptive filter, appropriate control signals to define the optimum MPPs can be extracted from the measured wind turbine system outputs.

### **Fig. 6. Performance of the adaptive filter**

## **8. “Fuzzy Logic” Optimal Power Point Tracking Controller**

The power loss in the electric generator is proportional to the generated power. As the electrical output is combined with the variation of mechanically stored energy in the rotating parts ( $\omega \cdot \dot{\omega} \cdot J$ ), power loss varies with the variation of mechanically stored energy. As the power loss increases when  $\omega \cdot \dot{\omega} \cdot J < 0$  and decreases when  $\omega \cdot \dot{\omega} \cdot J > 0$ , the effective power curve varies with variation of mechanically stored energy. The system needs to operate at the maximum point of the effective power curve to optimize energy harvesting. This is the optimum operating point of the combined

system of the wind rotor and the electric generator. The hill-climbing control criterion (presented in Fig. 7) can be followed to track the optimum power points for any  $\omega \cdot \dot{\omega} \cdot J$ . As the system parameters cannot be evaluated, exact relations between inputs and outputs of the system cannot be enumerated. Therefore, a “Fuzzy Logic” controller is introduced to optimize the performance of the system by considering qualitative parameters of filtered signals from the system outputs. At optimum operating point  $dP/d\omega = 0$  (see Fig. 7). The rotational speed of the wind rotor is controlled by varying the electrical load on the system. The value of  $dP/d\omega$  indicates the deviation of actual operating point from the optimum operating point and the value of  $\omega \cdot \dot{\omega} \cdot J$  indicates status of dynamics of the system. Therefore according to  $\omega \cdot \dot{\omega} \cdot J$  and  $dP/d\omega$ , the changing of wind rotor rotational speed step size can be modified for quicker response time to achieve the optimum operating point. Related “Fuzzy sets” and “Fuzzy rules” were developed by considering  $\omega \cdot \dot{\omega} \cdot J$  and  $dP/d\omega$  and are presented in Fig. 8 and Appendix (B) (where  $P = P_a - P_l$ ). The Centroid defuzzification method was used to obtain the “Fuzzy set” outputs ( $\Delta d$ ) [21]. A block diagram of the proposed Fuzzy Logic based MPPT controller is shown in Fig. 9.

### **Fig. 7 Control criteria**

The function of the MPPT is to provide the required load on the generator for optimum operation of the system. A schematic diagram of a small wind power system is shown in Fig. 10. By considering the Buck/Boost d.c.-d.c. converter (shown in Fig. 10), the voltage at d.c. bus ( $V_B$ ) is[22]:

$$V_B = V_G \left( \frac{D}{1-D} \right) \quad (28)$$

and the corresponding current flow towards the d.c. bus ( $I_B$ ) is[22]:

$$I_B = I_G \left( \frac{1-D}{D} \right) \quad (29)$$

where  $V_G$  is the voltage at the generator side and  $I_G$  is the current flow from the generator side. D is the duty ratio and varies between 0 to 1 according to[22]:

$$D = \left( \frac{T_{on}}{T_{on} + T_{off}} \right) \quad (30)$$

For a particular wind and rotational speeds, the output power is measured during time interval “t”. Then by varying the rate of change of ‘D’ ( $\Delta d$ ) and using “fuzzy logic”:

$$D_2 = D_1 + \Delta d \quad (31)$$

**Fig. 8 Related Fuzzy sets**

**Fig. 9 The proposed generic control system**

**Fig.10 A schematic diagram of a small wind power system**

## 9. Comparative Study

Performance of the proposed controller was compared with a controller employing a wind speed sensor, which is taken as a reference. The reference controller provides superior performance [2], as it respond quickly to wind speed variations. Normally, a proportional integrator (PI) controller is used to derive the maximum possible power from the wind at different wind speeds. An anemometer provides the reference signal to the MPPT controller which associates this to the turbine speed, rotor and generator

characteristics [23]. Variations of calculated optimal rotational speeds of the turbine, those obtained using the proposed controller and the reference controller with wind speed sensor are shown in Fig. 11. Optimal rotational speeds were determined based on the optimum operating points of the system by considering rotor & generator characteristics and wind speeds.

A wind turbine emulator was introduced in this study to evaluate the performance of the proposed controller and compare this with other control strategies. This is necessary to enable testing of the controllers' performance under different controlled conditions (including variable wind data) which are difficult to carry out in practice.

In the context of energy production, simulated results show that the proposed controller performs better than the controller based on a wind speed sensor. These results were verified by using a wind turbine emulator where a commercial DSP board (DS1103) from dSPACE was used to control the effective electric load on the generator. For a typical measured set of actual wind speed data, the energy captured over 2500 seconds period is 150,005 J with the proposed controller whilst that captured by using a controller with a wind speed sensor was 121,479 J. The test results show that the proposed generic optimal controller can capture 12% more energy from the available energy as compared to the wind speed sensor control method. Comparative results of the optimal control strategies are shown in Table 1. For the selected wind speed data, the amount of available energy over 2500 s period is 225,685 J. This can be expressed as:

$$\text{Available energy} = \sum_{\delta t=1}^{2500} \left[ \frac{1}{2} (\eta_{opt} \cdot \pi \cdot R^2 \cdot \rho \cdot C_{p\_opt} \cdot v^3) \delta t \right]$$

where  $\eta_{opt}$  is the generator efficiency and  $C_{p\_opt}$  is the power coefficient of the wind rotor at optimal operating conditions of the system for any wind speed.

**Table 1: Comparison results of optimal control strategies**

**Fig. 11 Comparison of turbine rotational speeds**

## 10. Conclusions

Accurate WECS characteristics are required when implementing conventional techniques for maximum power point tracking. However, WECSs are stochastic by nature and their characteristics vary from one system to another. The hill-climbing control technique (usually used with small-scale WECSs) operates by using measurements of electrical output power, without knowledge of system parameters. However, as described in this paper, for dynamic control in turbulent wind conditions, the electrical output power is weakly correlated with the input aerodynamic power. Consequently, it is difficult to determine the optimum operating points by using the hill-climbing technique, as variation of mechanically stored energy significantly affects the electrical power output.

Generally, small-scale WECSs have higher electrical losses due to higher winding resistance of small PMGs. Also, system losses during dynamic conditions are different from those at steady-state. Therefore, optimal operating points in steady-state conditions, which are considered in the wind sensor method, are not the same as those in dynamic state.

In this study, an Adaptive Filter is used to determine a signal representing the aerodynamic power that account for the dynamic conditions and system losses. This signal is used in conjunction with the hill climbing control method and results obtained showed improvement in system performance. Furthermore, a “Fuzzy Logic”

based hill-climbing control criterion is proposed to track the optimum operating points of the system by considering qualitative variation of the measured output parameters, without knowledge of system characteristics. The results obtained show that the proposed “generic” MPPT controller performs better than the wind sensor methods.

## 11. Appendices

### a. Specifications of the NERDC small wind turbine;

Rated capacity	: 200W
Radius of the wind rotor	: 1.105m
Number of blades	: 2
Moment of inertia of rotating parts (J)	: 9.77kg.m <sup>2</sup>
Generator	: Permanent magnet (3φ)
No. of pole pairs	: 6
Stator phase resistance	: 1.25Ω
Inductances [Ld, Lq]	: [0.003075H, 0.003075H]
Flux linkage by magnets	: 0.098V.s
Frictional factor	: 9.444×10 <sup>-15</sup> N.m.s

**b. Fuzzy rules;**

	If $\omega \cdot \dot{\omega} \cdot J$ is	and $dP/d\omega$ is	then $\Delta d$ is
1.	DH	DH	NC
2.	DL	DH	UM
3.	ST	DH	NC
4.	AL	DH	UM
5.	AH	DH	UH
6.	DH	DL	UM
7.	DL	DL	NC
8.	ST	DL	NC
9.	AL	DL	UL
10.	AH	DL	UM
11.	DH	ST	NC
12.	DL	ST	NC
13.	ST	ST	NC
14.	AL	ST	NC
15.	AH	ST	NC
16.	DH	AL	RM
17.	DL	AL	RL
18.	ST	AL	NC
19.	AL	AL	NC
20.	AH	AL	RM
21.	DH	AH	RH
22.	DL	AH	RM
23.	ST	AH	NC
24.	AL	AH	RM
25.	AH	AH	NC

## **12. Acknowledgment**

The authors would like to thank Northumbria University, New and Renewable Energy Centre (NaREC), UK and the National Engineering Research & Development Centre (NERDC), Sri Lanka for their support and providing the resources to conduct this project.

## **13. References**

- [1] E. Muljadi, K. Pierce, and P. Migliore, "Soft-control control for variable-speed stall-regulated wind turbines," *Wind Engineering*, vol. 85, pp. 277-291, 2000.
- [2] A. B. Jamal, V. Dinavahi, and A. Knight, "A review of power converter topologies for wind turbines," *Renewable Energy*, vol. 32, pp. 2369-2385, 2007.
- [3] S. Belakehal, H. Benalla, and A. Bentounsi, "Power maximization control of small wind system using permanent magnet synchronous generator," *Revue des Energies Renouvelables* vol. Vol. 12, pp. 307 – 319, 2009.
- [4] D. L. Gourieres, *Wind Power Plants Theory and Design*,: Oxford: Pergamon press, 1982.
- [5] T. Burton, D. Sharpe, N. Jenkins, and E. Bossanyi, *Wind Energy Handbook*: John Wiley & Sons, Ltd, 2001.
- [6] E. Muljadi, C. P. Butterfield, and Y. H. Wan, "Axial Flux, Modular, Permanent-Magnet Generator with a Toroidal Winding for Wind Turbine Applications," in *IEEE Industry Applications Conference* St. Louis, Mo, 1998.
- [7] M. A. Khan and P. Pillay, "Design of a PM Wind Generator, Optimised for Energy Capture over a Wide Operating Range," in *IEEE International Conference on Electric Machines and Drives*, 2005, pp. 1501-1506.

- [8] W. Leonhard, *Controls of Electrical drives*, 3rd ed.: Springer, Berlin Heidelberg New York, 2001.
- [9] L. Munteanu, A. L. Bratcu, N. A. Cutululis, and E. Ceanga, *Optimal Control of Wind Energy System: Towards a Global Approach*: Springer-Verlag London Limited, 2008.
- [10] M. Yin, G. Li, M. Zhou, and C. Zhao, "Modelling of the Wind Turbine with a Permanent Magnet Synchronous Generator for Integration," in *Power Engineering Society General Meeting IEEE*, 2007, pp. 1-6.
- [11] D. Grenier, L. A. Dessaint, O. Akhrif, Y. Bonnassieux, and B. Le Pioufle, "Experimental nonlinear torque control of a permanent-magnet synchronous motor using saliency," *Industrial Electronics, IEEE Transactions on*, vol. 44, pp. 680-687, 1997.
- [12] Md Arifujjaman, M T Iqbal, and J. E. Quaice, "Energy capture by a small wind-energy conversion system," *Applied Energy*, vol. 85, pp. 41-51, 2008.
- [13] S. Morimoto, H. Nakayama, M. Sanada and Y Takeda, "Sensorless output maximization control for variable-speed wind generation system using IPMSG," *IEE transaction on industry applications*, vol. 41, pp. 60-67, Jan/Fab 2005.
- [14] K. Tan and S. Islam, "Optimum Control Strategies in Energy Conversion of PMSG Wind Turbine System without Mechanical Sensors," *IEEE Transaction on Energy Conversion* vol. 19, pp. 392-399, June 2004.
- [15] T. Tanaka and T. Toumiya, "Output control by hill-climbing method for a small scale wind power generation system," *Renewable Energy*, vol. 12, pp. 387-400, 1997.
- [16] E. Koutroulis and K. Kalaitzakis, "Design of a Maximum Power Tracking

- System for Wind-Energy-Conversion Application," *IEEE Transaction on Industrial Electronics*, vol. 53, pp. 486-494, April 2006.
- [17] G. H. Riahy and M. Abedi, "Short term wind speed forecasting for wind turbine applications using linear prediction method," *Renewable Energy* vol. 33, pp. 35-41, 2008.
- [18] B. Widrow, J. R. Glover, Jr., J. M. McCool, J. Kaunitz, C. S. Williams, R. H. Hearn, J. R. Zeidler, Eugene Dong, Jr., and R. C. Goodlin, "Adaptive noise cancelling: Principles and applications," *Proceedings of the IEEE*, vol. 63, pp. 1692-1716, 1975.
- [19] G. C. Goodwin and K. S. Sin, *Adaptive filtering prediction and control*: Prentice hall, Inc, Englewood Cliffs, 1984.
- [20] S. Haykin, *Adaptive Filter Theory*: Prentice Hall, Englewood Cliffs, NJ, 1986.
- [21] T. J. Ross, *Fuzzy logic with engineering applications*: McGraw-Hill. Inc., 1995.
- [22] N. Mohan, T. M. Underland, and W. P. Robbins, *Power Electronics Converters, Application and Design* Third ed.: John Wiley and Sons, 2003.
- [23] Q. Wang and L. Chang, "An Intelligent Maximum Power Extraction Algorithm For Inverter-Based Variable Speed Wind Turbine Systems," *IEEE Transaction on power electronics*, vol. 19, pp. 1242-1249, September 2004.

## List of Tables

**Table 1: Comparison results of optimal control strategies**

## List of Figures

**Fig. 1. Wind rotor characteristics**

**Fig. 2. Operating point of the wind power system**

**Fig. 3. Function of MPPT mechanism**

**Fig. 4. Power flow of the wind turbine**

**Fig. 5. Function of the Adaptive filtering system**

**Fig. 6. Performance of the adaptive filter**

**Fig. 7. Control criteria**

**Fig. 8. Related Fuzzy sets**

**Fig. 9. The proposed generic control system**

**Fig.10 A schematic diagram of a small wind power system**

**Fig. 11 Comparison of turbine rotational speeds**

**Table 1: Comparison results of optimal control strategies**

<i>Optimal control strategies</i>	<i>Generated energy within 2500s (J)</i>	<i>As percentage of available energy (%)</i>
<i>Wind sensor method</i>	121478	53.8
<i>Proposed generic optimal controller</i>	150005	66.5

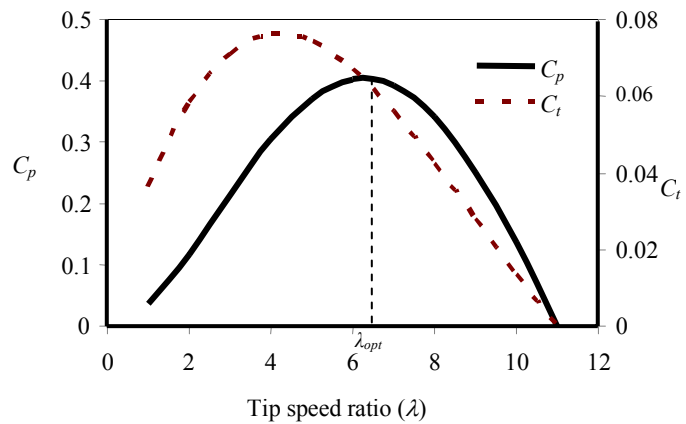


**Fig. 1. Wind rotor characteristics**

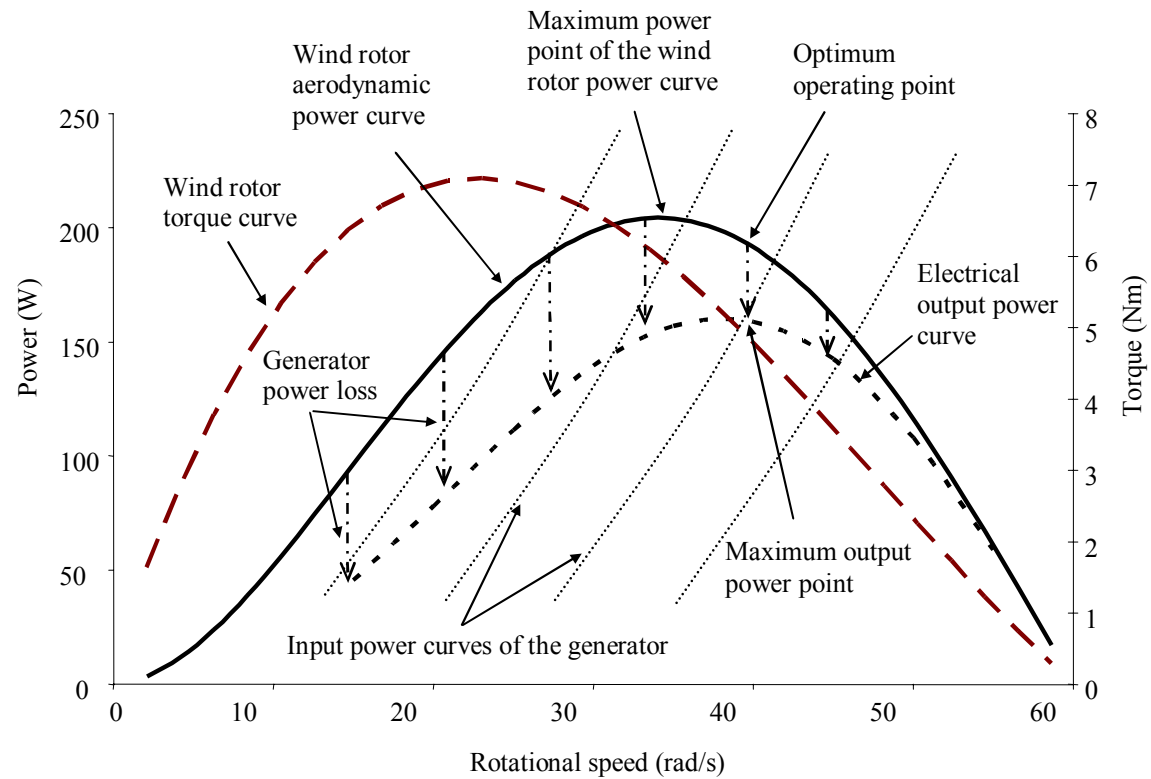


**Fig. 2. Operating point of the wind power system**

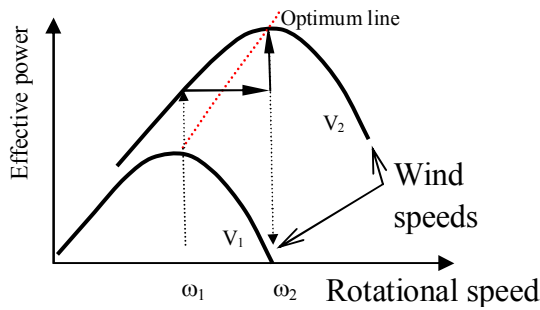


**Fig. 3. Function of MPPT mechanism**

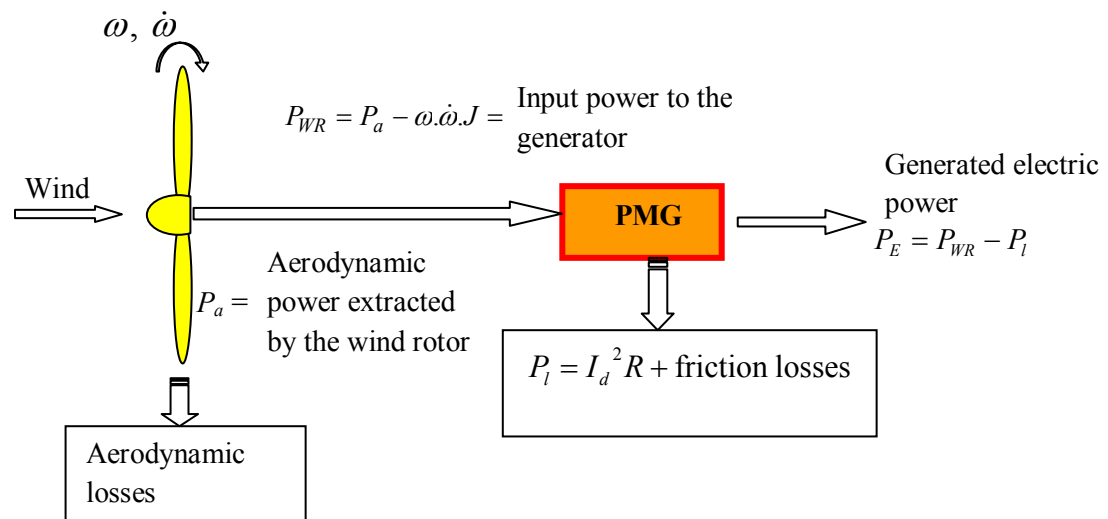


**Fig. 4. Power flow of the wind turbine**

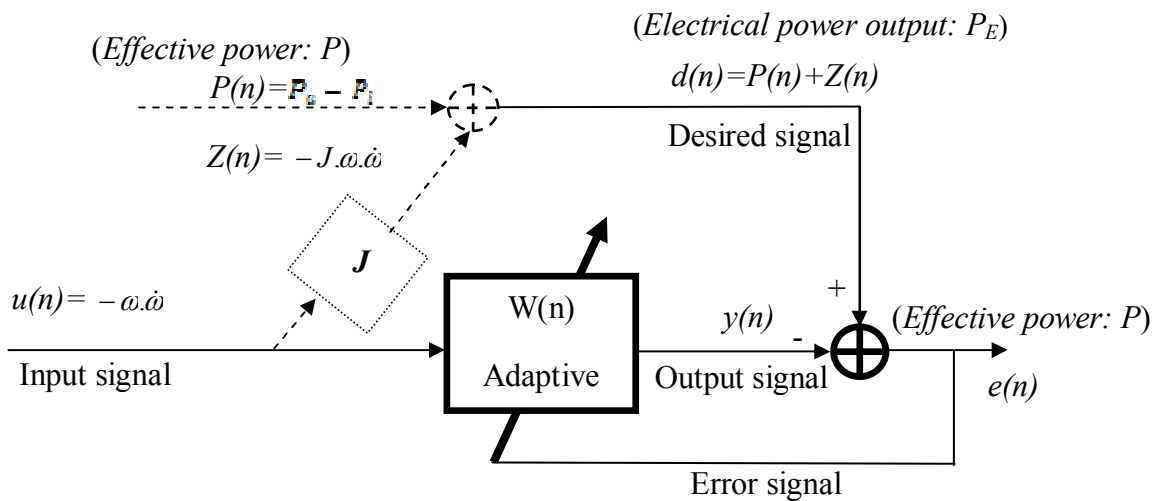


**Fig. 5. Function of the Adaptive filtering system**

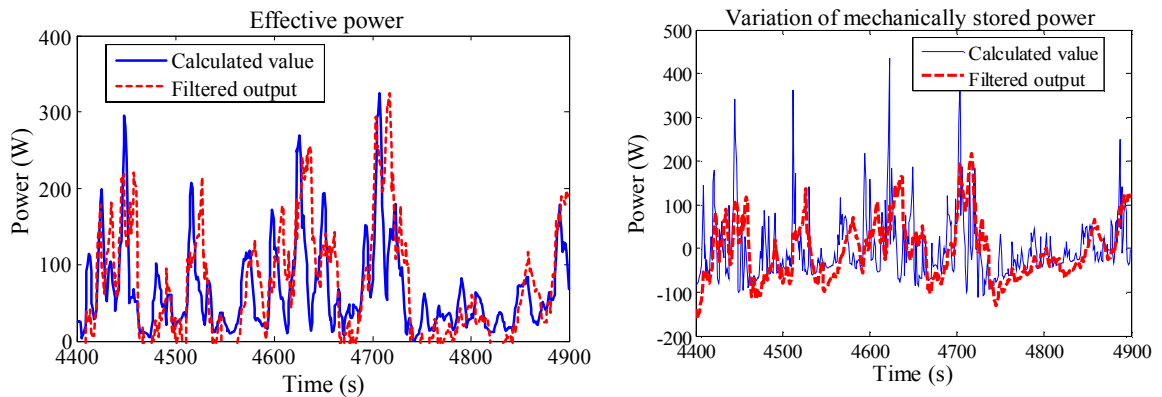


**Fig. 6. Performance of the adaptive filter**

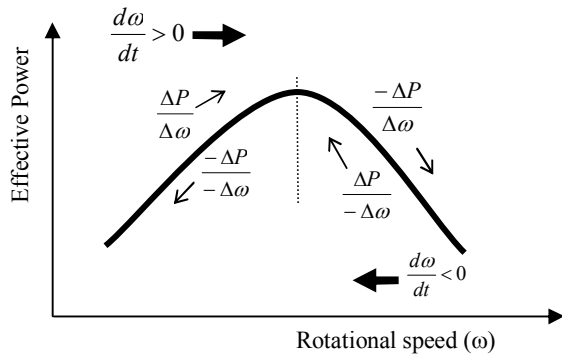


**Fig. 7. Control criteria**

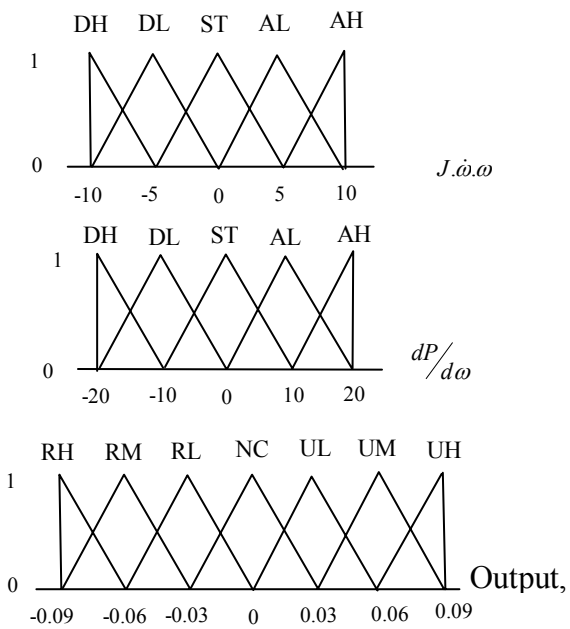


**Fig. 8. Related Fuzzy sets**

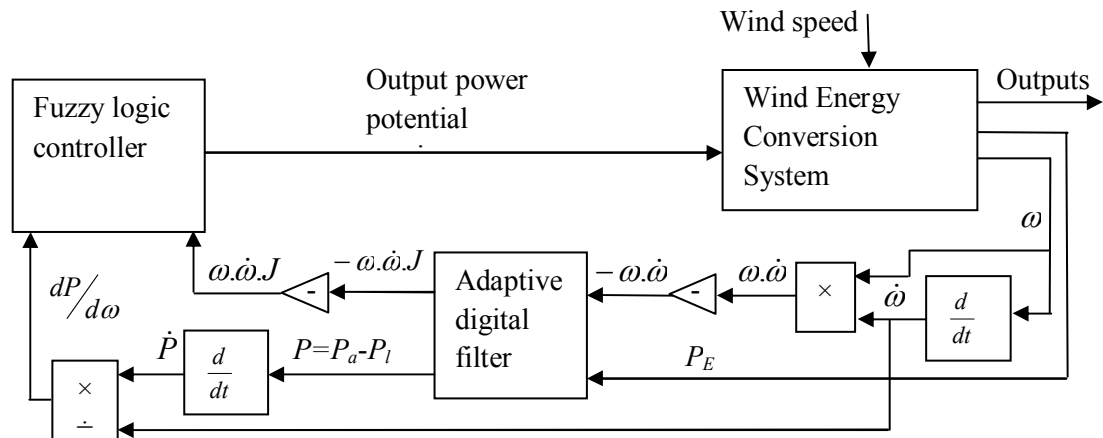


**Fig. 9. The proposed generic control system**

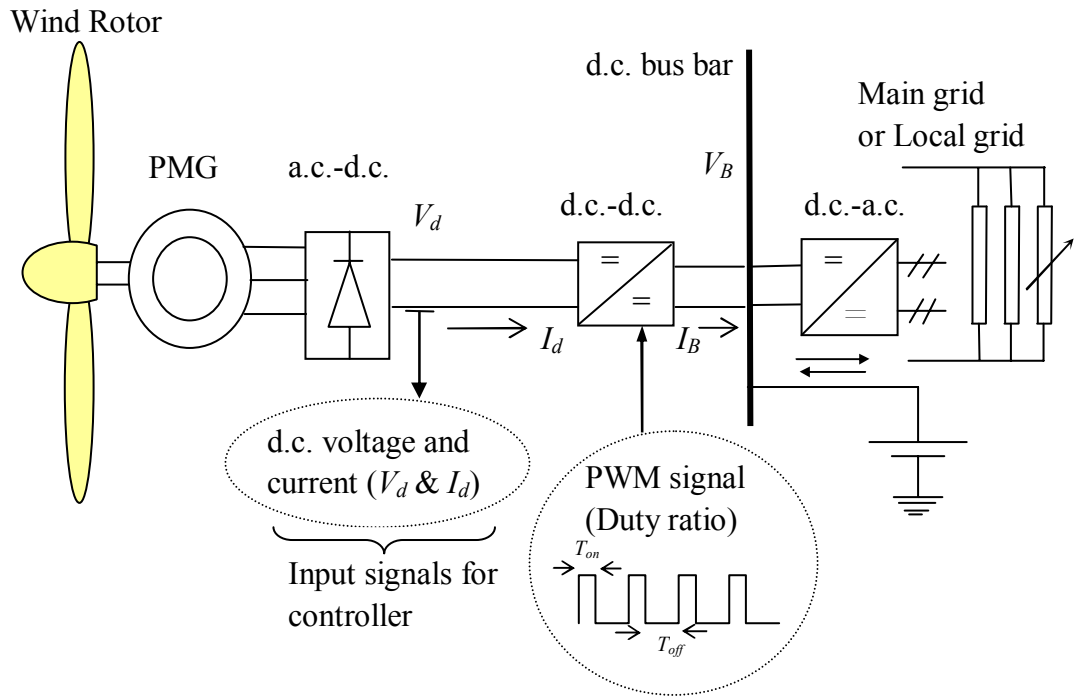


**Fig.10 A schematic diagram of a small wind power system**

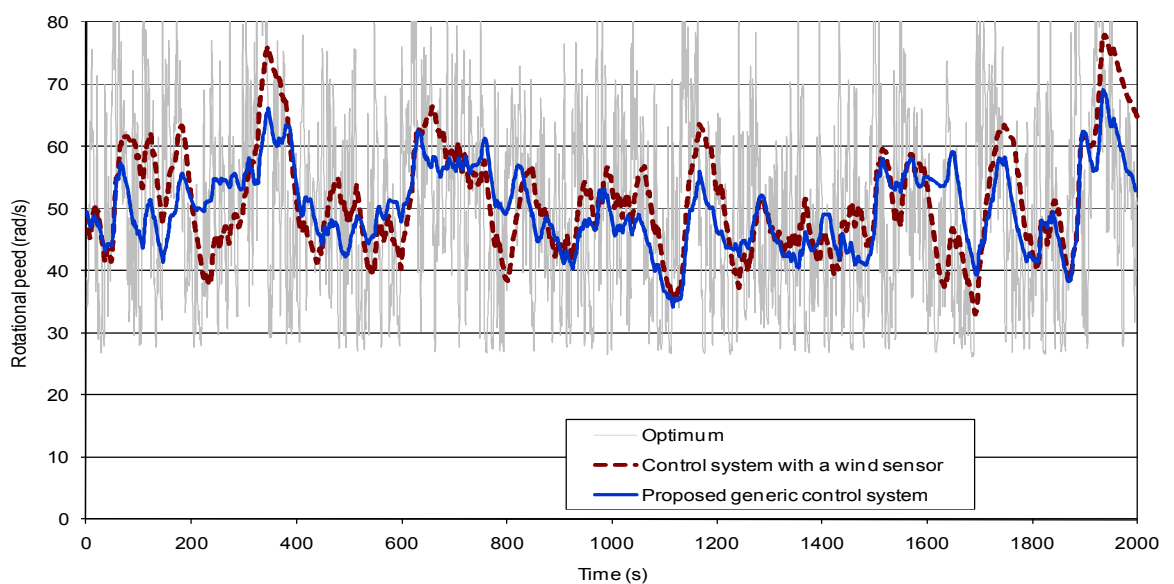


**Fig. 11 Comparison of turbine rotational speeds**